REDSHIFT DISTORTIONS AND CLUSTERING IN THE PSCZ SURVEY

W.E. BALLINGER[a], A.N. TAYLOR[b], A.F. HEAVENS[b], H. TADROS[a]
[a] *Department of Physics, Astrophysics, Keble Road, Oxford OX1 3RH, England,*
[b] *Institute for Astronomy, University of Edinburgh, Blackford Hill, Edinburgh EH9 3HJ, Scotland*

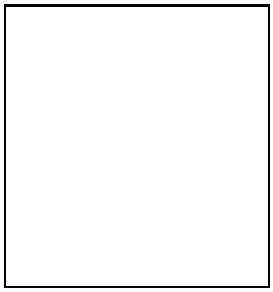

We have constrained the redshift-distortion parameter $\beta \equiv \Omega^{0.6}/b$ and the real-space power spectrum of the IRAS PSCz survey using a spherical-harmonic redshift-distortion analysis combined with a data compression method which is designed to deal with correlated parameters. Our latest result, $\beta = 0.4 \pm 0.1$, strongly rules out $\beta = 1$.

1 Introduction

It has been understood for a long time that redshift surveys are systematically distorted by peculiar velocities[11] – so called *redshift distortions*, which can cause the observed distribution of galaxies to become anisotropic. On large scales where linear theory applies, redshift distortions are characterised by the parameter[a] $\beta \equiv \Omega_{\rm m}^{0.6}/b$ – see Hamilton[8] for a detailed review.

In a classic paper, Kaiser[12] derived a simple formula for the effect of linear redshift distortions for a volume limited survey that subtends a small opening angle at the observer (the "distant observer" approximation – all lines of sight are treated as parallel). He showed that power is boosted by a factor $(1+\beta\mu_k^2)^2$, where μ_k is the cosine of the angle between wavevector and line of sight. Hamilton[6 7] and Cole, Fisher & Weinberg[4 5] analysed all-sky IRAS surveys using a method based on the Kaiser formalism, but were forced to break the survey up into sections because of the constraints of the distant observer approximation, losing information about the largest (and most reliably linear) scales.

Rather than fit a square peg into a round hole, Fisher *et al*[9] and Heavens & Taylor[10] (HT) dropped the plane parallel approximation and used a spherical harmonic decomposition to match the spherical nature of the IRAS redshift surveys. HT used spherical Bessel functions

[a] $\Omega_{\rm m}$ is the contribution to the density parameter from matter. The bias parameter b depends on galaxy type, in this paper it refers to IRAS galaxies.

to decompose the density field radially; using eigenfunctions of the Laplacian retains all the advantages of Fourier analysis. HT analysed the IRAS 1.2Jy survey, fitting β and the amplitude of the power spectrum; Ballinger, Heavens & Taylor[2](BHT) extended this analysis to fit the shape of the power spectrum. Tadros *et al*[18] (T99) applied these techniques to the IRAS PSCz survey – section 4 includes a review of those results.

2 Spherical Harmonic Formalism

We will briefly review the formalism for spherical harmonic analysis – see HT and T99 for details. The density field of the galaxy distribution $\rho(\mathbf{s})$ is expanded in terms of spherical harmonics, $Y_{\ell m}$, and a discrete set of spherical Bessel functions, j_ℓ,

$$\hat{\rho}_{\ell m n} = c_{\ell n} \int d^3s \, \rho(\mathbf{s}) w(s) j_\ell \left(k_{\ell n} s\right) Y^*_{\ell m} \left(\theta, \phi\right) , \tag{1}$$

where the $c_{\ell n}$ are normalization constants and k_{ln} are discrete wavenumbers.

These observed coefficients can be related to those of the true underlying density field ($\delta_{\ell m n}$) by:

$$\hat{\rho}_{\ell m n} = \left(\rho_0\right)_{\ell m n} + \sum_{\ell' m' n'} \sum_{n''} S^{n n''} W^{m m'}_{\ell \ell'} \left(\Phi^{n'' n'}_{\ell \ell'} + \beta V^{n'' n'}_{\ell \ell'}\right) \delta_{\ell' m' n'} . \tag{2}$$

The transition matrices $\mathbf{W}$, $\mathbf{\Phi}$, $\mathbf{V}$ and $\mathbf{S}$ describe the effects of the sky mask, the radial selection function, the linear redshift space distortion and the small scale distortion correction respectively; $\left(\rho_0\right)_{\ell m n}$ is a mean term, non-zero because of partial sky coverage. The transition matrices are derived and defined in HT and T99.

A likelihood approach is used to constrain β and the real-space power spectrum:

$$-2 \ln \mathcal{L}[\mathbf{D}|\beta, P(k)] = \ln(\det \mathbf{C}) + \mathbf{D}\mathbf{C}^{-1}\mathbf{D}^T, \tag{3}$$

where $\mathbf{C} = < \mathbf{D}\mathbf{D}^T >$ and elements of the data vector $\mathbf{D}$ are given by $D_{\ell m n} \equiv [\hat{\rho}_{\ell m n} - \left(\rho_0\right)_{\ell m n}]/\bar{\rho}$ where $\bar{\rho}$ is the mean number density – Gaussian statistics are assumed. Two different parameterisations of $P(k)$ are used: following HT a fixed shape is assumed and the amplitude is fitted, following BHT a stepwise maximum likelihood method is used, allowing the power spectrum to assume any shape (within bin discreteness).

3 Data – The IRAS PSCz Survey

The PSCz survey[14] is a redshift catalogue complete down to 0.6Jy over $\sim 83\%$ of the sky with a total of $\sim 15,000$ redshifts – it is the largest all sky survey in existence. As our method is very precise, we minimise systematic errors by using a more conservative flux cut (0.75Jy) and sky mask reducing the number of redshifts by a factor of roughly two – see T99.

4 Previous Results

Both the fixed amplitude (HT) and stepwise $P(k)$ (BHT) methods were applied to the PSCz by T99 for modes with $k \leq 0.13h$ Mpc^{-1}. The first method produced $\beta = 0.58 \pm 0.26$ and the amplitude of the real space power measured at wavenumber $k = 0.1h$ Mpc^{-1} of $\Delta_{0.1} = 0.42 \pm 0.03$ – see Fig. 2 (dashed contours). Freeing the shape of the power spectrum we find the consistent results $\beta = 0.47 \pm 0.16$ (conditional error), and $\Delta_{0.1} = 0.47 \pm 0.03$ – Fig. 1. T99 also carried out extensive tests on simulations, and the methods were found to be reliable. In addition, we carried out a suite of tests for systematics effects in the data and found the cut catalogue gave consistent results.

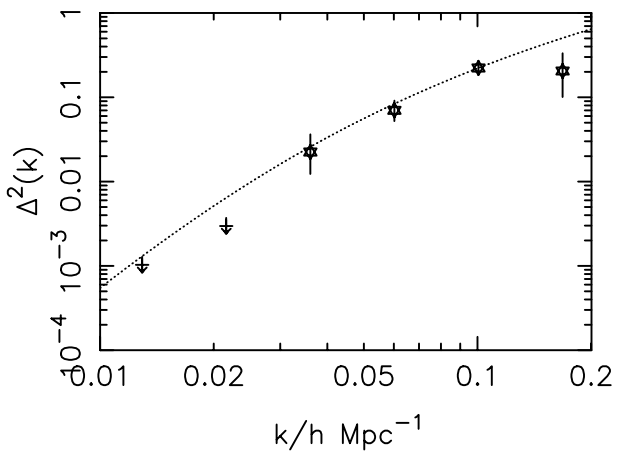

Figure 1: The real-space power spectrum of the PSCz redshift survey in dimensionless units (from T99). The curve is a CDM model with $\Gamma = 0.2$. The estimated value of β is 0.47 ± 0.16 (conditional error).

The method was restricted to a small range of wavenumber because the likelihood analysis involves the repeated inversion of a large $n \times n$ matrix; the time required for this process grows as n^3. More importantly, the matrix rapidly became numerically unstable. The results above do not strongly rule out either high (~ 1) or low (~ 0.5) values of β. It would be nice to overcome the matrix problem, extend the k-range and reduce the error bar.

5 Data Compression

It is possible to transform the (length n) data vector $\mathbf{D}$ to create a new, smaller dataset, while retaining most of the information about the parameters of interest[20]. A new dataset is constructed which is a linear combination of the original:

$$\mathbf{D}' = \mathbf{B}\mathbf{D}, \tag{4}$$

where $\mathbf{D}'$ is a new data vector of length $n' < n$, with a corresponding transformation for the covariance matrix. TTH show that the optimal matrix $\mathbf{B}$ which minimises the conditional error on a single parameter is made up from eigenvectors of[b]

$$\mathbf{C}_{,i}\,\mathbf{b} = \lambda \mathbf{C}\mathbf{b} \tag{5}$$

where the comma refers to a derivative with respect to parameter i. The new covariance matrix is smaller and also close to diagonal – hence much more stable.

TTH suggested extending this to multi-parameter problems by constructing a separate matrix $\mathbf{B}$ for each parameter and then using singular value decomposition to combine the matrices efficiently. However, Ballinger[1] (see also Taylor *et al*[19]) tested this and found that error ellipses / ellipsoids tended to grow along correlation axes – only conditional errors are constrained. Instead it was shown that equation (5) could be used to constrain the marginal errors by using one or more linear combinations of the original parameters which lie directly along the correlation axes.

Unfortunately solving equation (5) involves manipulating uncompressed $n \times n$ matrices. This usually isn't a timescale problem – it need only be done once – but still suffers from numerical difficulties. To avoid this problem, we split the data into several sections and compressed

[b] This, like the Wiener filter, is one of those marvellous data-handling methods which were invented by astronomers then sent back in time so that signal processing engineers could use them for the past fifty years.

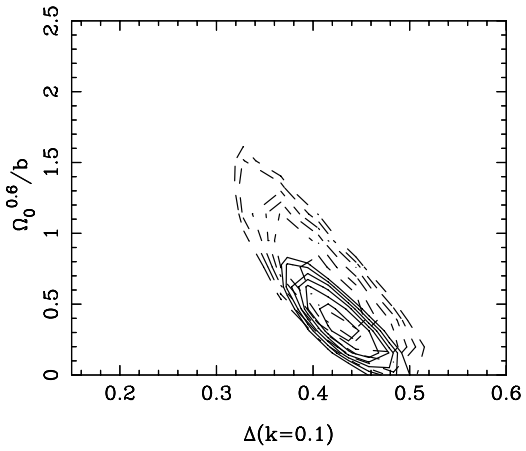

Figure 2: Likelihood contours for the two parameters $\beta = \Omega_0^{0.6}/b$ and the amplitude of the power spectrum for the PSCz survey. The new data-compression $k_{\max} = 0.2h$ Mpc^{-1} results (solid contours) are plotted along with the original $k_{\max} = 0.13h$ Mpc^{-1} results from T99 (dashed contours). Contours are plotted at intervals of $\delta \ln \mathcal{L} = 0.5$.

them separately, while still retaining full information about correlations between modes in different sections. Strictly speaking this is slightly less optimal than compressing the whole dataset in one go, but it should make a negligible difference in practice and will not bias the result.

6 New Results and conclusions

Fig. 2 shows the old $k_{\max} = 0.13h$ Mpc^{-1} result together with the new $k_{\max} = 0.2h$ Mpc^{-1} obtained using data compression. The original 4644 modes were compressed down to 2278. The new, lower, value of $\beta = 0.4 \pm 0.1$ is consistent with the previous result but the error ellipse is considerably smaller; the best-fit amplitude of the power spectrum is essentially unchanged. $\beta = 1$, corresponding to $\Omega_{\rm m} = 1$, $b = 1$, is now strongly disfavoured. More details will be in Ballinger *et al* and Taylor *et al* (in preparation).

The low value of β is consistent with currently popular cosmological models with a low value of $\Omega_{\rm matter}$ if the IRAS bias parameter is close to unity. The value is somewhat lower than that from other analyses of the PSCz survey[3 13 15 16], but not inconsistent. It is consistent with the recent *velocity-velocity* comparison results from peculiar velocity catalogues[22], but somewhat lower than the corresponding *density-density* value[17]. See Willick[21] for a discussion.

References

1. W.E. Ballinger, PhD thesis, University of Edinburgh, 1997.
2. W.E. Ballinger, A.F. Heavens and A.N. Taylor, MNRAS **276**, 59P (1995) (BHT).
3. E. Branchini *et al* MNRAS **308**, 1 (1999).
4. S. Cole, K.B. Fisher and D.H. Weinberg, MNRAS **267**, 785 (1994).
5. S. Cole, K.B. Fisher and D.H. Weinberg, MNRAS **275**, 515 (1995).
6. A.J.S. Hamilton, ApJ **385**, L5 (1992).
7. A.J.S. Hamilton, ApJ **406**, L47 (1993).
8. A.J.S. Hamilton in *The Evolving Universe, Ringberg Workshop on Large-Scale Structure 1996*, ed. D. Hamilton (Kluwer Academic, Dordrecht, 1998), (astro-ph/9708102).
9. K.B. Fisher, C. Scharf and O. Lahav, MNRAS **266**, 219 (1994).
10. A.F. Heavens and A.N. Taylor, MNRAS **275**, 483 (1995) (HT).
11. J. Jackson, MNRAS **156**, 1P (1972).
12. N. Kaiser, MNRAS **227**, 1 (1987).

13. M. Rowan-Robinson *et al* (astro-ph/9912223).
14. W. Saunders *et al*, (astro-ph/0001117).
15. I. Schmoldt *et al*, MNRAS **304**, 893 (1999).
16. I. Schmoldt *et al*, AJ **118**, 1146 (1999).
17. Y. Sigad, A. Eldar, A. Dekel, M. Strauss and A. Yahil, ApJ **495**, 516 (1998).
18. H. Tadros *et al*, MNRAS **305**, 527 (1999) (T99).
19. A.N. Taylor, A.F. Heavens, W.E. Ballinger and M. Tegmark, (astro-ph/9707265).
20. M. Tegmark, A.N. Taylor and A.F. Heavens, ApJ **480**, 22 (1997).
21. J. Willick, these proceedings, (astro-ph/0003232)
22. J. Willick, M. Strauss, A. Dekel and T. Kolatt, ApJ **486**, 629 (1997).